Chemical Science

ROYAL SOCIETY OF CHEMISTRY

EDGE ARTICLE

View Article Online
View Journal | View Issue

Open Access Article. Published on 21 November 2023. Downloaded on 1/25/2026 10:50:51 AM. This article is licensed under a Creative Commons Attribution-NonCommercial 3.0 Unported Licence.

Check for updates

Cite this: *Chem. Sci.*, 2023, **14**, 14262

All publication charges for this article have been paid for by the Royal Society of Chemistry

Received 21st August 2023
Accepted 19th November 2023

DOI: 10.1039/d3sc04390h

rsc.li/chemical-science

# An orbitally adapted push–pull template for $N_2$ activation and reduction to diazene-diide†

David Specklin, Marie-Christine Boegli, Anaïs Coffinet, Léon Escomel, Laure Vendier, Mary Grellier and Antoine Simonneau *

A Lewis superacidic bis(borane) $C_6F_4\{B(C_6F_5)_2\}_2$ was reacted with tungsten $N_2$-complexes $[W(N_2)_2(R_2PCH_2CH_2PR_2)_2]$ (R = Ph or Et), affording zwitterionic boryldiazenido W(II) complexes *trans*-$[W(L)(R_2PCH_2CH_2PR_2)_2(N_2\{B(C_6F_5)_2(C_6F_4B(C_6F_5)_3\})]$ (L = ø, $N_2$ or THF). These compounds feature only one N–B linkage of the covalent type, as a result of intramolecular boron-to-boron $C_6F_5$ transfer. Complex *trans*-$[W(THF)(Et_2PCH_2CH_2PEt_2)_2(N_2\{B(C_6F_5)_2C_6F_4B(C_6F_5)_3\})]$ (**5**) was shown to split $H_2$, leading to a seven-coordinate complex $[W(H)_2(Et_2PCH_2CH_2PEt_2)_2(N_2\{B(C_6F_5)_2\}_2C_6F_4)]$ (**7**). Interestingly, hydride storage at the metal triggers backward $C_6F_5$ transfer. This reverts the bis(boron) moiety to its bis(borane) state, now doubly binding the distal N, with structural parameters and DFT computations pointing to dative N→B bonding. By comparison with an $N_2$ complex $[W(H)_2(Et_2PCH_2CH_2PEt_2)_2(N_2\{B(C_6F_5)_3\})]$ (**10**) differing only in the Lewis acid (LA), namely $B(C_6F_5)_3$, coordinated to the distal N, we demonstrate that two-fold LA coordination imparts strong $N_2$ activation up to the diazene-diide ($N_2^{2-}$) state. To the best of our knowledge, this is the first example of a neutral LA coordination that induces reduction of $N_2$.

## Introduction

Dinitrogen activation by transition-metals as a means to transform this inert molecule under mild conditions has attracted the interest of chemists for almost 60 years.[1] Over the last five decades, dinitrogen complexes of the d-,[1] f-[2] and recently s-[3] and p-[4] block elements have been described in the literature, exhibiting a wealth of coordination modes, oxidation states and reactivity for the $N_2$ ligand. Some have shown potential as greener alternatives[5] to the energy- and fossil fuel-intensive Haber–Bosch process,[6] or for the synthesis of value-added (organo)nitrogen compounds.[7] They can serve as models of the nitrogen-fixing enzymes nitrogenases, that feature an organometallic FeM (M = Mo, V or Fe) cofactor that can bind the diatomic molecule.[8] Interaction of dinitrogen with a transition metal is well described by the Chatt–Dewar–Duncanson model:[9] the metal centre "pushes" its d-electrons into the antibonding orbitals of $N_2$. High activation may ultimately be reached in dinuclear edifices through "push–push" activation.[1b,10] "Push–pull" activation of dinitrogen[11] remains less explored. It consists of enhancing the polarization of dinitrogen when coordinated to a metal centre through non-covalent interaction with an electron-deficient species,[12] mimicking to a certain extent the effect of secondary-sphere H-bonding between $N_2$ and the multiple acidic functions of nitrogenases' active site.[12f,i,13,14] Several groups have evidenced that a single non-covalent interaction of a neutral transition-metal[12a] or main group[12b–g,j] Lewis acid (LA), an alkali[12f,h] or $Au(I)^+$ cation[12j] or a weak acid[12i] (neutral or charged) leads to enhanced activation of $N_2$ thanks to augmented charge transfer (Fig. 1). A parallel between push–pull activation and the chemistry of frustrated Lewis pairs (FLPs)[15] can be drawn, since the reactivity thereof resides in the synergistic action of a strong LA *pulling* electron density and a bulky Lewis base *pushing* its electron pair into antibonding orbitals of a substrate to activate. The chemistry of FLP still lacks a genuine $N_2$ capture example,[16] but the Stephan group has proposed the $B(C_6F_5)_3$ adduct of diphenyldiazomethane as a model thereof (Fig. 1).[17,18] The above-mentioned body of work thus provides clues of what to expect from push–pull or FLP-related $N_2$ activation in terms of structure, whereas the higher polarization of the $N_2$ unit in these compounds may ultimately lead to the discovery of new reactivity.[12f,19] Besides, the N≡N→LA linkage may show FLP-type reactivity, such as Si–H bond heterolytic splitting, resulting in $N_2$ silylation.[12g,20] Of note, the analogous reaction employing $H_2$ for N–H bond formation[21] is yet to be achieved and is challenged by the propensity of $H_2$ to easily substitute $N_2$.[22] Alternatively, $[R_3XH]^+[R'_3BH]^-$ (X = N or P) ion pairs delivered by FLP $H_2$ splitting[23] have been employed to protonate $N_2$.[24,25]

Main-group Lewis acids interact with a molecular orbital of an $N_2$ complex that mixes a filled metal's d orbital and a π*

*LCC-CNRS, Université de Toulouse, CNRS, UPS, 205 route de Narbonne, BP44099, F-31077 Toulouse Cedex 4, France. E-mail: antoine.simonneau@lcc-toulouse.fr*

† Electronic supplementary information (ESI) available: Synthetic protocols, spectroscopic characterization, DFT computations, and CIF files. CCDC 2115061, 2115062, 2115063, 2115066 and 2285830. For ESI and crystallographic data in CIF or other electronic format see DOI: https://doi.org/10.1039/d3sc04390h



© 2023 The Author(s). Published by the Royal Society of Chemistry

Open Access Article. Published on 21 November 2023. Downloaded on 1/25/2026 10:50:51 AM.
This article is licensed under a Creative Commons Attribution-NonCommercial 3.0 Unported Licence.

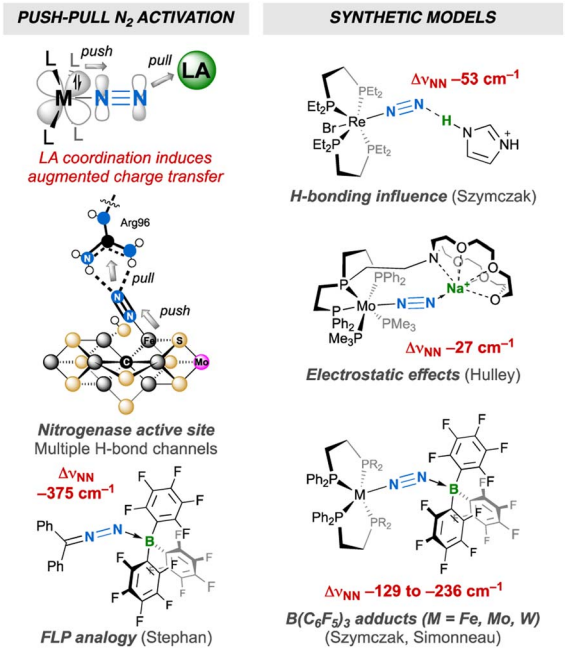


Fig. 1 $N_2$ push–pull activation: bioinorganic relevance, FLP analogy and synthetic models.

orbital of $N_2$.[12f,j,26] To the best of our knowledge, the two-fold coordination of a neutral LA to the distal N was never reported,[27,28] although it would be interesting to judge how far the resulting push–pull effect affects the $N_2$ unit when compared to two-fold protonation[24a,29] or functionalisation,[30] without being altered by the association of the conjugated base or leaving group with the metal that generally takes place in the two former cases. Such an achievement would also complement previous studies aimed at measuring the push–pull influence of monotopic LAs,[12] showing how multiple electron-deficient centres (as found in nitrogenases' active sites) may synergistically enhance $N_2$ activation. To this end, we have explored the coordination of a strongly electrophilic bis(borane) to a terminal $N_2$ complex (Fig. 1) and endeavour to compare the push–pull effect with the one induced by $B(C_6F_5)_3$. We hoped that the two empty p orbitals of the tethered B atoms would spatially match with the two lobes of the distal N's p orbital. Such an "orbitally adapted" push–pull template should result in high $N_2$ activation and polarisation as a result of greater stabilization of the d+π* frontier orbital (Fig. 2). In this article, we show that particular conditions should be met to observe two-fold coordination of the bis(borane). Indeed, hydride storage through $H_2$ oxidative addition at the metal–$N_2$ complex was key to achieve this goal, allowing us to discover that LA adducts of group 6 $N_2$ complexes may react with $H_2$ without $N_2$ loss (but not through FLP-type splitting). It is shown that two-fold LA coordination exerts a very strong influence on the diatomic molecule, and comparison of structural, spectroscopic and computational data supports its activation up to the 2-e$^-$ reduced state.

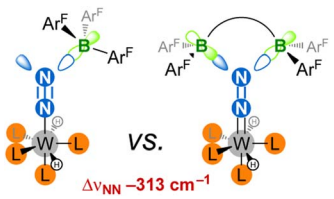


Fig. 2 This work: achievement of two-fold LA coordination on an $N_2$ ligand results in an extreme push–pull effect. $Ar^F = C_6F_5$.

## Results and discussion

When we reacted equimolar amounts of the dinitrogen complexes $[W\{R_2P(CH_2)_2PR_2\}_2(N_2)_2]$ ($\mathbf{1^R}$ with R = Ph or Et, $Ph_2P(CH_2)_2PPh_2$ = dppe and $Et_2P(CH_2)_2PEt_2$ = depe) with the Lewis superacidic[31] bis(borane) $C_6F_4$-1,2-$\{B(C_6F_5)_2\}_2$ (**2**) reported by the Piers group,[32] the rapid crystallization at room temperature of a new species $[W(dppe)_2(N_2\{B(C_6F_5)_2C_6F_4B(C_6F_5)_3\})]$ **3** in moderate yield was observed (Scheme 1), whereas a depe analogue *trans*-$[W(N_2)(depe)_2(N_2\{B(C_6F_5)_2C_6F_4B(C_6F_5)_3\})]$ **4** was obtained in high yield from a $PhF/C_6H_6$ mixture. Complexes **3** and **4** were found to be poorly soluble in toluene-$d_8$ or $C_6D_6$ and decomposed readily in $CD_2Cl_2$ or PhCl-$d_5$. When dissolved in THF-$d_8$, complex **3** converted immediately to a mixture of compounds whose identification was made difficult due to rapid polymerization of the medium. In the same solvent, **4** cleanly turns to a THF complex *trans*-$[W(THF)(depe)_2(N_2\{B(C_6F_5)_2C_6F_4B(C_6F_5)_3\})]$ (**5**) after $N_2$ substitution, as evidenced by visible gas evolution. The latter could be isolated in high yield after removal of solvent under vacuum. Generation of **5** in a 1 : 1

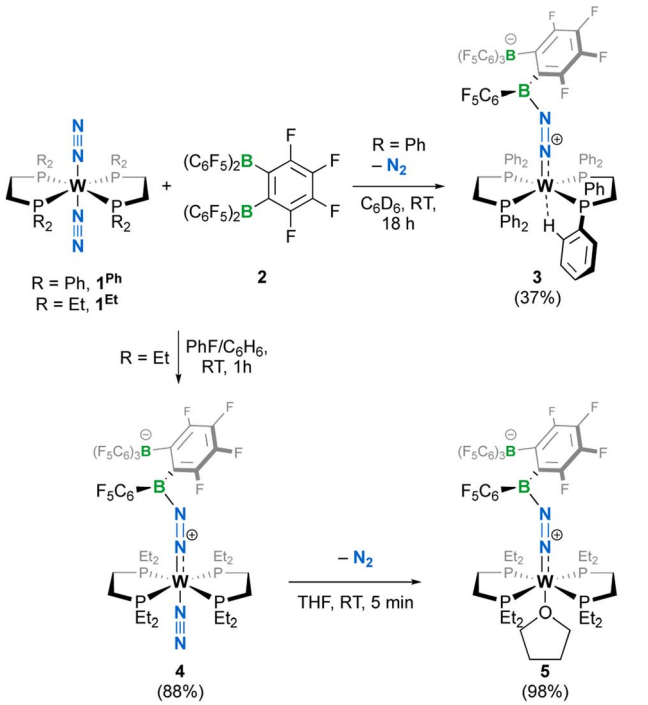


Scheme 1 Syntheses of complexes **3–5**; isolated yields in parentheses.

© 2023 The Author(s). Published by the Royal Society of Chemistry

Open Access Article. Published on 21 November 2023. Downloaded on 1/25/2026 10:50:51 AM. This article is licensed under a Creative Commons Attribution-NonCommercial 3.0 Unported Licence.

reaction of **2** and $\mathbf{1}^{\mathbf{Et}}$ in THF was not optimal as THF polymerization occurred upon solvation of the reactants. Complex **5** has been characterized in solution by $^{1}$H, $^{31}$P, $^{19}$F and $^{11}$B NMR spectroscopy. The $^{1}$H and $^{31}$P NMR were diagnostic of two pairs of inequivalent phosphine ligands with two pseudo-singlets in $^{31}P\{^{1}H\}$ NMR at 38.6 and 33.8 ppm, with $^{2}J_{PP}$ inferred by 2D experiments but too weak (<1 Hz) to be resolved (Fig. S5†). In $^{11}$B NMR (Fig. S6†), only a well resolved borate resonance was observed as a singlet at −15.05 ppm, indicating boron quaternarization. The other resonance could not be detected even at high concentrations, presumably as a consequence of quadrupolar coupling in an unfavourable electric field gradient situation that leads to fast relaxation of the nuclei.[33] In $^{19}$F NMR, all fluorine atoms were found to be magnetically inequivalent (Fig. S8†). We surmised that steric crowding of the bis(borane) moiety might result in hindered rotation of $C_6F_5$ substituents at the NMR time scale, thus differentiating the fluorine nuclei.

The crystalline materials afforded in the above-mentioned reactions could be analysed by single crystal X-ray diffraction (sc-XRD), but the obtained structures for **5** were of too poor quality to be discussed. The solid-state structures of the spectroscopically similar complexes **3** and **4** reveal that the bis(borane) moiety interacts with the terminal nitrogen *via* a single boryl centre through covalent, double B–N bonding (Fig. 3). These are the first examples of dinitrogen borylation where the $BR_2$ group is sourced from a triarylborane.[34,35] The second boron atom is found as a tetraaryl borate centre, in agreement with boron NMR analysis. This $\kappa^1$B arrangement of the bis(boron) moiety results from a $C_6F_5$ transfer, similar to what was observed upon methyl abstraction on $[Cp_2Zr(CH_3)_2]$ by **2** to form the anion $[B(Me)(C_6F_5)(C_6F_4\{B(C_6F_5)_3\}]$,[32c] and likely occurs as a means to mitigate steric repulsion between the $C_5F_6$ groups and the phosphines' substituents. The boron atoms are essentially coplanar with the bridging $C_6F_4$ group, but steric tension in these edifices is revealed by the two boron centres being pushed away from each other, with C–C–B angles in the phenylene junctions approaching 130°. Meanwhile, the borate moiety significantly deviates from the ideal tetrahedral geometry. Short W–N distances (**3**: 1.788(3); **4**: 1.860(6) Å) and long N–N ones (**3**: 1.248(5); **4**: 1.249(8) Å) suggest a formal W=N=N motif, and the *trans* effect from the second $N_2$ ligand in **4** is likely to be responsible for the elongated W–N distance compared to that of **3**. Whereas infrared spectroscopy did not allow us to clearly identify the boryldiazenido N–N bond stretches (see Fig. S1–S3 and S9, S10†), which was not surprising given the elongated $N_2$ unit found in **3** and **4**, resonance Raman spectroscopy of **5** shows an intense line in the spectrum at 1364 $cm^{-1}$ (Fig. S11†). $^{15}$N isotopic enrichment shifts this line to 1343 $cm^{-1}$ (Fig. S12†). These frequencies agree with a N=N linkage as they are close to those of the $\nu_{NN}$ of azo-dyes (*ca.* 1400 $cm^{-1}$).[37] A weak band observed at 2220 $cm^{-1}$ in the IR spectrum of **4** was attributed to the terminal $N_2$ ligand. The bent N–N–B angles (*ca* 140°) are typically found in other examples of boryldiazenido–tungsten complexes.[12g,20a,b,28,33a,b,38] The B–N bonds are *ca.* 1.40 Å long, indicative of significant double B–N bonding. Collectively, these parameters point to a formal description of these compounds as W(II)-boryldiazenido complexes. Interestingly, the main compositional difference between **3** and **4** is also found when comparing the adducts of $B(C_6F_5)_3$ with $\mathbf{1}^{\mathbf{Ph}}$[12g] or $\mathbf{1}^{\mathbf{Et}}$[12j]: in complex **3** the *trans* coordination site features an agostic interaction involving the $C_{ortho}$–H of a phenyl substituent of the dppe ligand, whereas the depe analogue **4** retains its second $N_2$ ligand. We believe that the relative instability of **3** originates from the labile agostic bond that may expose the Lewis acidic, 16-electron tungsten centre to further reactivity. Because we failed to observe double coordination of the bis(borane) to the terminal $N_2$ ligand of complexes $\mathbf{1}^{\mathbf{R}}$, we briefly explored the reactivity of **5** (Scheme 2). The instability of **3** in common solvents precluded such study. Among the various tests we have carried out, the reaction with dihydrogen was particularly rewarding in view of our initial goal. Treating **5** with $H_2$ produced almost immediately a new complex $[W(H)_2(depe)_2(N_2\{B(C_6F_5)_2C_6F_4B(C_6F_5)_3\})]$ (**6**) that readily decomposed upon attempting its isolation by concentration under vacuum. The $^{31}$P NMR points to the occurrence of two isomers for **6**, possibly due to a hindered free rotation induced by the bulkiness of the bis(boron) moiety (Fig. S14†). Each shows four similar signals, indicative of a dissymmetry of the first coordination sphere. The $^{11}$B NMR spectrum is basically unchanged. Over the course of several days, **6** evolves upon heating into a new species $[W(H)_2(depe)_2(N_2\{B(C_6F_5)_2\}_2C_6F_4)]$ (**7**) for which the $^{11}$B NMR spectrum shows significant change in the bis(boron) moiety (disappearance of the borate signal at $\delta$ = −15.1 ppm and a new, deshielded resonance at −3.4 ppm). Yellow crystals of **7** could be recovered and analysed by sc-XRD (Fig. 4), revealing oxidative addition of $H_2$ and the seven-coordinate nature of **7** with one isomerized depe ligand.[39] Remarkably, the bis(borane) pairs with the basic terminal N through two-fold single, dative-type bonding (B–N distances are *ca.* 1.61 *vs. ca.* 1.40 Å for **4**) of its two boron atoms after

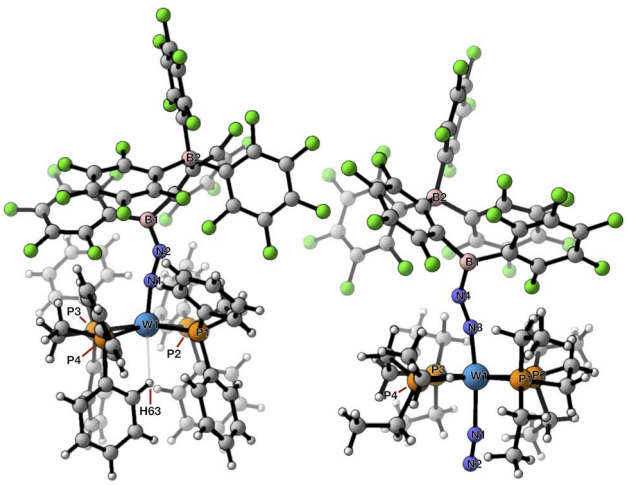


Fig. 3 Molecular structures of complexes **3** (left) and **4** (right) in the solid state rendered with CYLview20.[36] Selected distances (Å) and angles (°): **3**: W1–H63 2.437, W1–N1 1.788(3), N1–N2 1.248(5), N2–B1 1.400(5), W1–N1–N2 168.9(3), N1–N2–B1 141.7(4); **4**: W1a–N1 2.155(7), N1–N2 1.117(11), W1a–N3 1.860(6), N3–N4 1.249(8), N4–B1 1.368(10), W1a–N1–N2 171.5(8), W1a–N3–N4 165.3(5), N3–N4–B1 143.9(6).


© 2023 The Author(s). Published by the Royal Society of Chemistry

Open Access Article. Published on 21 November 2023. Downloaded on 1/25/2026 10:50:51 AM.
This article is licensed under a Creative Commons Attribution-NonCommercial 3.0 Unported Licence.

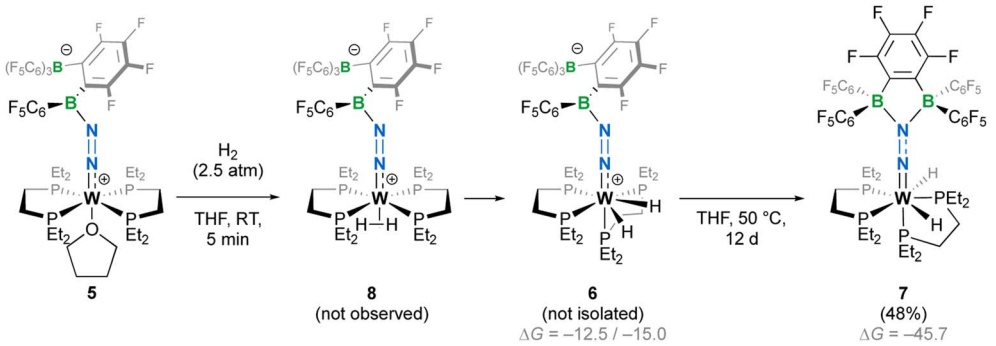


Scheme 2 Reaction of **5** with dihydrogen leading to seven-coordinate complexes **7**. Isolated yields in parentheses. Δ*G* (DFT, B3PW91-6-31G(d,p)) are given in kJ mol$^{-1}$.

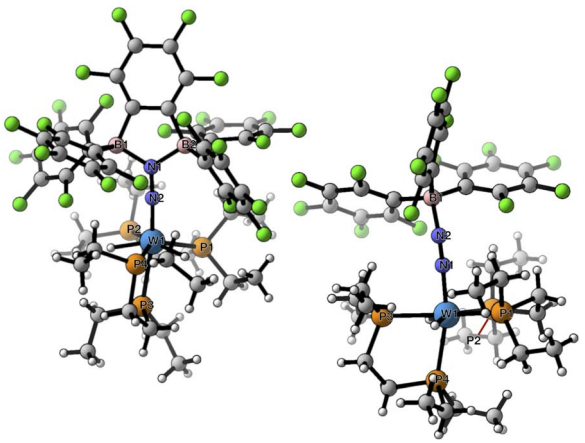

Fig. 4 Molecular structures of complexes **7** (left) and **10** (right) in the solid state. Selected distances (Å) and angles (°): **7**: W1–P1 2.559(1), W1–P2 2.516(1), W1–P3 2.651(1), W1–P4 2.475(1), W1–N2 1.825(2), N1–N2 1.291(3), N1–B1 1.615(3), N1–B2 1.614(3), W1–H100 1.66(3), W1–H200 1.62(2), W1–N2–N1 177.0(2), N2–N1–B1 125.0(2), N2–N1–B2 121.8(2), B1–N1–B2 113.3(2). **10**: W1–P1 2.4813(5), W1–P2 2.4792(5), W1–P3 2.4300(5), W1–P4 2.5214(5), W1–N1 1.8826(17), N1–N2 1.193(2), N1–B1 1.562(3), W1–H1 1.71(3), W1–H2 1.70(3), W1–N1–N2 167.21(15), N1–N2–B1 139.13(18).

a backward $C_6F_5$ transfer. This results in augmented, push–pull type charge transfer to the $N_2$ ligand, as shown by the remarkably long N–N bond of 1.291(3) Å, going beyond that of a N–N double bond.[40] As a specific comparison, N–N bond lengths of two-fold 1,2-B($C_6F_5$)$_3$ adducts of diazene ($N_2H_2$, 1.230(3) Å) and diazenide ($N_2H^-$, 1.2227(18) Å))[41] or LA adducts of diazenes (1.227(2)–1.263(4) Å) are much shorter.[42] To the best of our knowledge, this is the first example of a neutral adduct of an end-on $N_2$ ligand with a ditopic Lewis acid.

DFT calculations were conducted to shed light on this transformation (see Fig. S40†). Structure optimization allowed us to locate a *trans*-σ-$H_2$ complex **8** and a more stable *cis*-dihydride that could well correspond to **6**. Two rotamers (**6** and **6′**) were found for the latter species, whose energy difference matches well with the experimentally observed ratio. Isomer **7** was found to be more stable than **6** by 31 kJ mol$^{-1}$. Estimates of $^1$H chemical shifts for the W-bound protons that we were not able to locate in the $^1$H NMR spectra (see Fig. S13 and S18†) were also computed. They fall within the alkyl protons' region and probably overlap with the resonances linked to the phosphine's substituents (see Plot S1†), supporting the absence of resonances at higher fields.

The activation of dihydrogen by **5** pushed us to verify whether a simpler system, that is the adduct of B($C_6F_5$)$_3$ with $\mathbf{1^{Et}}$, *trans*-[W($N_2$)(depe)$_2$($N_2${B($C_6F_5$)$_3$}] (**9**), would react similarly—a positive result would also provide a comparison of the influence of a mono- *vs.* di-topic LA to $N_2$ activation. Gratifyingly, under an $H_2$ atmosphere, **9** evolved into the bis-hydride complex [W(H)$_2$(depe)$_2$($N_2${B($C_6F_5$)$_3$}] (**10**) without $N_2$ loss. We were able to isolate it in high yields and carried out its full characterization. We could not evidence FLP-type heterolytic splitting of $H_2$ at the B–N linkage, similar to what we observed when we reacted an adduct of $\mathbf{1^{Ph}}$ and B($C_6F_5$)$_3$ with hydroboranes and -silanes.[12g] Here, dihydrogen favoured reactivity at the reduced metal centre. sc-XRD analysis of **10** revealed a similar first coordination sphere to that of **7** (Fig. 4). The influence of dihydrogen oxidative addition on $N_2$ activation may be measured by comparing **10** with the adduct of B($C_6F_5$)$_3$ with $\mathbf{1^{Et}}$ (**9**).[12j] The two structures are rather similar (Table 1), with a slightly higher activation level for $N_2$ in **10** (1.196(2) *vs.* 1.179(9) Å for **9**). This is also reflected by the IR stretching frequencies (1767 cm$^{-1}$ for **9** *vs.* 1712 cm$^{-1}$ for **10**). The N–N–B angle is also more acute in **10**, which may be due to reduced steric hindrance of the isomerized first coordination sphere (Table 1). Interestingly, **7** could also be obtained from **10** in high yields by simply reacting it with one equivalent of bis(borane) **2** (Scheme 3), with B($C_6F_5$)$_3$ being displaced upon slight thermal activation.

Comparison of the structures of the $N_2$ complexes **7** and **10** supports the depiction of the $N_2$ unit in **7** as a diazene-diide ($N_2^{2-}$) ligand (Table 1): as mentioned above, the N–N bond length (1.291(3) Å) goes beyond that of standard N–N double bonds. The linearisation of the W–N–N array in **7** (177 *vs.* 167° for **10**) and the significant shortening of the W–N bond (1.82 *vs.* 1.88 Å for **10**) are also in line with the diatomic molecule being an LX-type ligand. In addition, the smaller N–N–B angles point to a fully sp$^2$-hybridized distal nitrogen, as expected for the $N_2^{2-}$ dianion. $^{15}$N labelling of **7** and **10** allowed us to unambiguously

Open Access Article. Published on 21 November 2023. Downloaded on 1/25/2026 10:50:51 AM. This article is licensed under a Creative Commons Attribution-NonCommercial 3.0 Unported Licence.

Table 1 Comparison of pertinent structural parameters, NN stretching frequencies. Values in parentheses were calculated by DFT (B3PW91, 6-31G(d,p), and D3BJ). Computed infrared frequencies were corrected with a scaling factor = 0.958. n.a. = not applicable. n.d. = not determined. as = asymmetric. s = symmetric

| Bonds (Å)/angles (°)/$\nu$ ($cm^{-1}$) | $\mathbf{1}^{Et}$[a] | 9[a] | 10 | 7 |
|---|---|---|---|---|
| W–N (theor.) | 2.016 | 1.908(6) | 1.883(2) *(1.873)* | 1.825(2) *(1.831)* |
| N–N (theor.) | 1.123(2) | 1.179(9); 1.08(1) | 1.193(2) *(1.184)* | 1.291(3) *(1.243)* |
| N–B (theor.) | n.a. | 1.55(1) | 1.562(3) *(1.556)* | 1.615(1) *(1.626[0])*[b] |
| W–$P_{trans}$ (theor.) | n.a. | n.a. | 2.5214(5) *(2.512)* | 2.651(1) *(2.609)* |
| W–N–N (theor.) | 178.6(1) | 169.0(6) | 167.2(2) *(166.8)* | 177.0(2) *(175.9)* |
| N–N–B (theor.) | n.a. | 148.4(7) | 139.1(2) *(135.3)* | 123.4(23) *(123.6[18])*[b] |
| av. N–W–$P_{eq}$[b] | 90.0(9) | 91(4) | 89(4) | 99(6) |
| $\nu_{NN}$ $^{14}N$ (theor.)/$^{15}N$[c] | 1890/1830 (as) | 1767 | 1712 *(1827)*/1659 | 1399 *(1548)*/1338 |
| $\nu_{NN}$ $^{14}N/^{15}N$[d] | 1968/1903[e] (s) | n.d. | 1714/1664 | Not observed |

[a] Taken from ref. 12*j*. [b] Averaged data; standard deviation calculated from the measurement set are not the average of the standard deviation of individual measurements. [c] FT-ATR infrared spectroscopy. [d] Resonance Raman spectroscopy. [e] Taken from ref. 43.

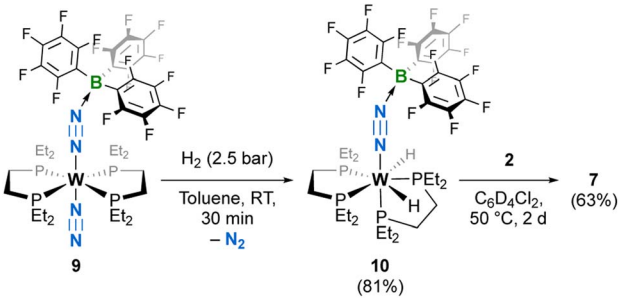


Scheme 3 Synthesis of bis-hydride **10** by the reaction of $H_2$ with the $B(C_6F_5)_3$ adduct of $\mathbf{1}^{Et}$, **9**, and displacement of the borane by bis(borane) **2** to give **7**. Isolated yields in parentheses.

locate N–N stretches in their IR spectra (Table 1, Fig. S22, S23 and S31, S32†). Surprisingly, no shifting lines could be observed when comparing the Raman spectra of $^{14}N$- and $^{15}N$-**7** (Fig. S24 and S25†), while in the case of **10**, a low-intensity line at 1714 $cm^{-1}$ shifted to 1664 $cm^{-1}$ for the $^{15}N$ isotopologue (Fig. S33 and S34†). The strong bathochromic shift recorded for the stretching frequency of **7** (1399 *vs.* 1712 $cm^{-1}$ for **10**) and the structural data indeed support the $N{=}N^{2-}$ depiction.[37,40–42] The reaction of **10** with **2** points to diborane coordination-triggered 2-$e^-$ reduction of $N_2$, and somewhat recalls the evolution of the N–N bond upon the two-fold protonation of related group 6 $N_2$ complexes affording hydrazido complexes.[29] The resulting positively charged compounds show N–N bond lengths ranging from 1.30–1.37 Å depending on the *trans* ligand and H-bonding in the lattice. Interestingly, the Schrock group was, to the best of our knowledge, the only group to report structural data for both Mo-diazenido and Mo-hydrazido complexes, the latter being obtained by protonation of the former. Surprisingly, the N–N bond lengths are equal for these two compounds (1.302(13) *vs.* 1.304(6), respectively). Although this single point of comparison prevents a general conclusion to be drawn, it is remarkable that in our case, the effect of incremental LA coordination is much more pronounced. Unfortunately, comparison of $^{15}N$ NMR chemical shifts could not be performed since despite several hours of acquisition, we were not able to detect resonances for **7** (see Fig. S7, S17 and S29† for the $^{15}N$ NMR spectra of **5**, **6** and **10**, respectively).

DFT calculations including dispersion (D3BJ) were run on **7** and **10** (see the ESI for details and atomic coordinates of the computed structures). Key metrical parameters were found to be close to those experimentally determined or within the margin of error of DFT (Table 1). Comparison of the atomic charges obtained by a Natural Population Analysis (NPA) evidences that the negative charge carried by the $N_2$ unit in **7** (−0.46) is 1.5 times higher than that found in **10** (−0.30). In both cases, it is almost totally localized on the distal nitrogen, in agreement with previous observations,[12f] and the N–N bond in **7** is significantly more polarised. A much higher negative charge is carried by the metal atom in **10**, in line with a diminished metal-to-$N_2$ charge transfer and a lower formal oxidation state attributed to its W centre. Wiberg bond indices (WBI) also reflect the trends revealed by the structures of **7** and **10**: a higher N–N WBI is found in **10** (1.94 *vs.* 1.57 in **7**, Fig. 5), but a lower W–N one (1.23 *vs.* 1.50 in **7**). As far as the B–N bonds are concerned, a smaller N–B WBI in **7** parallels the longer N–B distances found in its crystal structure (Table 1). Analysis of the Natural Bonding Orbitals (NBOs) further differentiates **7** and **10**. In **10**, the W–N bonding involves

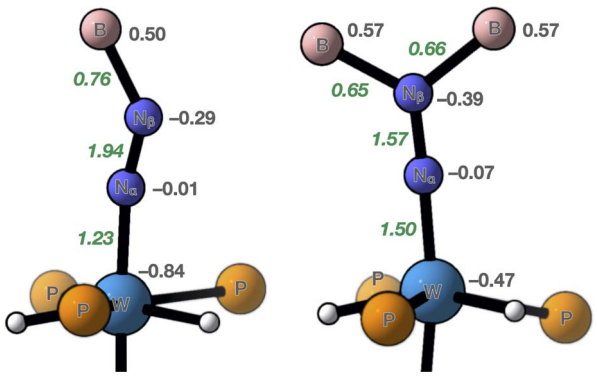


Fig. 5 Summary of key parameters from theoretical calculations run on **7** (right) and **10** (left). Grey figures are NPA charges and green italic ones, Wiberg bond indices.


© 2023 The Author(s). Published by the Royal Society of Chemistry

Open Access Article. Published on 21 November 2023. Downloaded on 1/25/2026 10:50:51 AM. This article is licensed under a Creative Commons Attribution-NonCommercial 3.0 Unported Licence.

mainly atomic orbitals of σ symmetry, while for **7** it is computed to rest on π-symmetric orbitals exclusively (see Fig. S51–S53† for visualization of key pNBOs and Natural Localized Molecular Orbitals [NLMOs] of **7** and **10**). In both cases, the W–N NBO is polarized towards the nitrogen atom. Interestingly, a lone pair is found on the proximal nitrogen of **7**, which undergoes significant stabilizing donor–acceptor interactions with the W–$P_{trans}$ antibond. This is where the W–N σ-symmetric bonding lies, and this is what explains why in **7** the W–$P_{trans}$ bond is significantly elongated compared to that of **10** (Table 1). In other terms, it translates the stronger *trans* influence of the diazene-diide ligand. Conversely, **10** carries a lone pair of pure d character on W for which second-order perturbation theory estimates an important stabilization by a donor–acceptor interaction with a π* of $N_2$, thus embodying π back-donation. Moving to the N–N linkage, a single π bond is found for **7** along the σ component, whereas **10** has two, indicating an intact triple N–N linkage, unlike **7**. N–B NBOs are polarised towards nitrogen to the same extent in both compounds (*ca.* 75%), yet the natural atomic hybrids on nitrogen differ significantly from **7** to **10**, reflecting $sp^2$ and sp hybridization, respectively (see Tables S7 and S8† for a summary of pertinent values issued by NBO analysis). Collectively, these computational observations also support a 2-$e^-$ reduced $N_2$ unit, stabilised by a W(IV) centre through σ and π donation from the nitrogen ligand, as well as by two-fold dative N→B bonding in **7**.

## Conclusions

We have explored the coordination of the strongly electrophilic bis(borane) **2** to terminal dinitrogen complexes $[W\{R_2P(CH_2)_2PR_2\}_2(N_2)_2]$ ($\mathbf{1^R}$) with the hope to observe $\kappa^2$B coordination to the distal nitrogen, thus building an orbitally adapted push–pull template for $N_2$ activation. The reaction with either $\mathbf{1^{Ph}}$ or $\mathbf{1^{Et}}$ did not furnish the expected outcome with formation of covalent N–B bonds in complexes *trans*-$[W(L)(R_2PCH_2CH_2PR_2)_2(N_2\{B(C_6F_5)_2(C_6F_4B(C_6F_5)_3\})]$ (L = ø, $N_2$ or THF) (**3–5**) after boron-to-boron $C_6F_5$ transfer. The reactivity of *trans*-$[W(THF)(depe)_2(N_2\{B(C_6F_5)_2C_6F_4B(C_6F_5)_3\})]$ (**5**) with dihydrogen was then explored. It triggered backward $C_6F_5$ transfer upon oxidative addition of $H_2$, without $N_2$ loss, and afforded complex $[W(H)_2(depe)_2(N_2\{B(C_6F_5)_2\}_2C_6F_4)]$ (**7**) having the bis(borane) coordinating the distal nitrogen *via* two-fold dative bonding. Its especially long N–N bond (1.29 Å) goes beyond reference N=N distances (1.21–1.25 Å). The $B(C_6F_5)_3$ analogue of **7**, complex $[W(H)_2(depe)_2(N_2\{B(C_6F_5)_3\}]$ (**10**), could be prepared by oxidative addition of $H_2$ on adduct $[W(N_2)(depe)_2(N_2\{B(C_6F_5)_3\}]$ **9**. In **10**, $B(C_6F_5)_3$ can be displaced by bis(borane) **2** to furnish **7**. Comparison of **7** with **10** led us to propose that the $N_2$ ligand underwent 2$e^-$ reduction upon coordination of the bis(borane), due to an extreme push–pull effect. To the best of our knowledge, this is the first example of LA-coordination-induced reduction of an $N_2$ ligand, a transformation that is commonly observed upon protonation or functionalisation.[29,30] This points to a possible strong influence of the multiple H-bonding channel when $N_2$ is coordinated to the FeMo cofactor of the nitrogenases. Guidelines for future $N_2$ fixation FLP systems may also be drawn from our study as we demonstrate that bis(borane) can trigger reduction of the diatomic molecule when combined to an electron-rich species, a reactivity commonly observed in small molecule activation by FLPs. Future work will focus on the reactivity of **7** and **10**, new complexes that have the rare but remarkable ability to activate $N_2$ and $H_2$ at a single metal centre;[22d,44] promoting N–H bond formation in such species should be facilitated by the proximity of the two hydrides with the $N_2$ ligand.[45]

## Data availability

All the relevant curated data can be found in the ESI† as stated in the footnote. Raw data were not uploaded into repositories.

## Author contributions

D. S., M.-C. B., A. C. and L. E. run the experiments and analyzed the data. L. V. recorded single-crystal X-ray diffraction data and solved the structures. M. G. performed DFT calculations and assisted in the writing of the manuscript. A. S. obtained funding for the project and managed it, conceived the original idea, designed the experiments and took part in the analysis of the data. D. S. wrote the preliminary manuscript draft and A. S. took charge of writing the submitted and revised versions. D. S., M.-C. B., M. G. and A. S. were involved in the writing of the ESI.† All authors were involved in the proof-reading process.

## Conflicts of interest

There are no conflicts to declare.

## Acknowledgements

The authors would like to thank Pr. François P. Gabbaï, Dr Mitsukimi Tsunoda and Dr Kirill I. Tugashov for providing expert advice on the synthesis of $[HgC_6F_4]_3$ necessary to prepare bis(borane) **2**. D. S., M.-C. B. and A. S. are indebted to the European Research Council for funding (ERC Starting Grant no 757501). A. C. is grateful to the French Ministry of National and Superior Education and Research (MENESR) for a PhD fellowship. This work was partly supported by the ANR PUNCh project (post-doc fellowship for L. E.), grant ANR-21-CE07-0003 of the French Agence Nationale de la Recherche.

## References

1 (*a*) F. Masero, M. A. Perrin, S. Dey and V. Mougel, *Chem.–Eur. J.*, 2021, **27**, 3892–3928; (*b*) D. Singh, W. R. Buratto, J. F. Torres and L. J. Murray, *Chem. Rev.*, 2020, **120**, 5517–5581; (*c*) *Transition Metal-Dinitrogen Complexes: Preparation and Reactivity*, ed. Y. Nishibayashi, Wiley-VCH Verlag GmbH & Co. KGaA, Weinheim, Germany, 2019; (*d*) R. J. Burford and M. D. Fryzuk, *Nat. Rev. Chem*, 2017, **1**, 1–13; (*e*) M. D. Walter, in *Advances in Organometallic Chemistry*, ed. P. J. Pérez, Elsevier, 2016, vol. 65, pp. 261–377.

Open Access Article. Published on 21 November 2023. Downloaded on 1/25/2026 10:50:51 AM. This article is licensed under a Creative Commons Attribution-NonCommercial 3.0 Unported Licence.

2 (*a*) Y. Tanabe, in *Transition Metal-Dinitrogen Complexes*, 2019; (*b*) Z. R. Turner, *Inorganics*, 2015, **3**, 597–635; (*c*) M. G. Gardiner and D. N. Stringer, *Materials*, 2010, **3**, 841–862; (*d*) W. J. Evans and D. S. Lee, *Can. J. Chem.*, 2005, **83**, 375–384.

3 (*a*) B. Rösch, T. X. Gentner, J. Langer, C. Färber, J. Eyselein, L. Zhao, C. Ding, G. Frenking and S. Harder, *Science*, 2021, **371**, 1125–1128; (*b*) R. Mondal, K. Yuvaraj, T. Rajeshkumar, L. Maron and C. Jones, *Chem. Commun.*, 2022, **58**, 12665–12668.

4 (*a*) M.-A. Légaré, G. Bélanger-Chabot, R. D. Dewhurst, E. Welz, I. Krummenacher, B. Engels and H. Braunschweig, *Science*, 2018, **359**, 896–900; (*b*) M.-A. Légaré, M. Rang, G. Bélanger-Chabot, J. I. Schweizer, I. Krummenacher, R. Bertermann, M. Arrowsmith, M. C. Holthausen and H. Braunschweig, *Science*, 2019, **363**, 1329–1332; (*c*) M.-A. Légaré, G. Bélanger-Chabot, M. Rang, R. D. Dewhurst, I. Krummenacher, R. Bertermann and H. Braunschweig, *Nat. Chem.*, 2020, **12**, 1076–1080; (*d*) S. Bennaamane, B. Rialland, L. Khrouz, M. Fustier-Boutignon, C. Bucher, E. Clot and N. Mézailles, *Angew. Chem., Int. Ed.*, 2023, **62**, e202209102.

5 (*a*) Y. Tanabe and Y. Nishibayashi, *Chem. Soc. Rev.*, 2021, **50**, 5201–5242; (*b*) Q. J. Bruch, G. P. Connor, N. D. McMillion, A. S. Goldman, F. Hasanayn, P. L. Holland and A. J. M. Miller, *ACS Catal.*, 2020, **10**, 10826–10846; (*c*) M. J. Chalkley, M. W. Drover and J. C. Peters, *Chem. Rev.*, 2020, **120**, 5582–5636; (*d*) S. L. Foster, S. I. P. Bakovic, R. D. Duda, S. Maheshwari, R. D. Milton, S. D. Minteer, M. J. Janik, J. N. Renner and L. F. Greenlee, *Nat. Catal.*, 2018, **1**, 490–500; (*e*) N. Stucke, B. M. Flöser, T. Weyrich and F. Tuczek, *Eur. J. Inorg. Chem.*, 2018, **2018**, 1337–1355; (*f*) *Nitrogen Fixation*, ed. Y. Nishibayashi, Springer International Publishing AG, Cham, Switzerland, 2017; (*g*) Y. Roux, C. Duboc and M. Gennari, *ChemPhysChem*, 2017, **18**, 2606–2617.

6 (*a*) M. Appl, *Ammonia, 2. Production Processes*, 2011; (*b*) G. Ertl, *Angew. Chem., Int. Ed.*, 2008, **47**, 3524–3535; (*c*) J. W. Erisman, M. A. Sutton, J. Galloway, Z. Klimont and W. Winiwarter, *Nat. Geosci.*, 2008, **1**, 636; (*d*) R. Schlögl, *Angew. Chem., Int. Ed.*, 2003, **42**, 2004–2008; (*e*) V. Smil, *Enriching the Earth: Fritz Haber, Carl Bosch, and the Transformation of World Food Production*, Mit Press, 2001; (*f*) V. Smil, *Nature*, 1999, **400**, 415; (*g*) J. R. Jennings, *Catalytic Ammonia Synthesis: Fundamentals and Practice*, Springer, New York, 1991.

7 (*a*) S. Kim, F. Loose and P. J. Chirik, *Chem. Rev.*, 2020, **120**, 5637–5681; (*b*) Z.-J. Lv, J. Wei, W.-X. Zhang, P. Chen, D. Deng, Z.-J. Shi and Z. Xi, *Natl. Sci. Rev.*, 2020, **7**, 1564–1583.

8 (*a*) O. Einsle and D. C. Rees, *Chem. Rev.*, 2020, **120**, 4969–5004; (*b*) L. C. Seefeldt, Z.-Y. Yang, D. A. Lukoyanov, D. F. Harris, D. R. Dean, S. Raugei and B. M. Hoffman, *Chem. Rev.*, 2020, **120**, 5082–5106; (*c*) B. M. Hoffman, D. Lukoyanov, Z.-Y. Yang, D. R. Dean and L. C. Seefeldt, *Chem. Rev.*, 2014, **114**, 4041–4062; (*d*) K. Tanifuji and Y. Ohki, *Chem. Rev.*, 2020, **120**, 5194–5251.

9 D. Dubois and R. Hoffmann, *Nouv. J. Chim.*, 1977, **1**, 479–492.

10 S. Gambarotta and J. Scott, *Angew. Chem., Int. Ed.*, 2004, **43**, 5298–5308.

11 (*a*) A. Coffinet, A. Simonneau and D. Specklin, in *Encyclopedia of Inorganic and Bioinorganic Chemistry*, ed. R. A. Scott, Wiley-VCH Verlag GmbH & Co. KGaA, 2020, pp. 1–25; (*b*) A. J. Ruddy, D. M. C. Ould, P. D. Newman and R. L. Melen, *Dalton Trans.*, 2018, **47**, 10377–10381; (*c*) A. Simonneau and M. Etienne, *Chem.–Eur. J.*, 2018, **24**, 12458–12463.

12 (*a*) J. Chatt, J. R. Dilworth, R. L. Richards and J. R. Sanders, *Nature*, 1969, **224**, 1201–1202; (*b*) J. Chatt, R. H. Crabtree and R. L. Richards, *J. Chem. Soc. Chem. Commun.*, 1972, 534; (*c*) J. Chatt, R. H. Crabtree, E. A. Jeffery and R. L. Richards, *J. Chem. Soc. Dalton Trans.*, 1973, 1167–1172; (*d*) F. Studt, B. A. MacKay, S. A. Johnson, B. O. Patrick, M. D. Fryzuk and F. Tuczek, *Chem.–Eur. J.*, 2005, **11**, 604–618; (*e*) H. Broda, S. Hinrichsen, J. Krahmer, C. Nather and F. Tuczek, *Dalton Trans.*, 2014, **43**, 2007–2012; (*f*) J. B. Geri, J. P. Shanahan and N. K. Szymczak, *J. Am. Chem. Soc.*, 2017, **139**, 5952–5956; (*g*) A. Simonneau, R. Turrel, L. Vendier and M. Etienne, *Angew. Chem., Int. Ed.*, 2017, **56**, 12268–12272; (*h*) L. G. Pap, A. Couldridge, N. Arulsamy and E. Hulley, *Dalton Trans.*, 2019, **48**, 11004–11017; (*i*) J. P. Shanahan and N. K. Szymczak, *J. Am. Chem. Soc.*, 2019, **141**, 8550–8556; (*j*) D. Specklin, A. Coffinet, L. Vendier, I. del Rosal, C. Dinoi and A. Simonneau, *Inorg. Chem.*, 2021, **60**, 5545–5562.

13 (*a*) P. C. Dos Santos, R. Y. Igarashi, H.-I. Lee, B. M. Hoffman, L. C. Seefeldt and D. R. Dean, *Acc. Chem. Res.*, 2005, **38**, 208–214; (*b*) T. Spatzal, K. A. Perez, O. Einsle, J. B. Howard and D. C. Rees, *Science*, 2014, **345**, 1620–1623; (*c*) S. M. Keable, J. Vertemara, O. A. Zadvornyy, B. J. Eilers, K. Danyal, A. J. Rasmussen, L. De Gioia, G. Zampella, L. C. Seefeldt and J. W. Peters, *J. Inorg. Biochem.*, 2018, **180**, 129–134; (*d*) D. Sippel, M. Rohde, J. Netzer, C. Trncik, J. Gies, K. Grunau, I. Djurdjevic, L. Decamps, S. L. A. Andrade and O. Einsle, *Science*, 2018, **359**, 1484–1489; (*e*) W. Kang, C. C. Lee, A. J. Jasniewski, M. W. Ribbe and Y. Hu, *Science*, 2020, **368**, 1381–1385. Although the structural data reported in this latter reference have been the matter of a discussion, the role of acidic residues in the nitrogenases' active site for $N_2$ activation remains a solid hypothesis, see ref. 8*a*–*c* and 13*a*.(*f*) J. W. Peters, O. Einsle, D. R. Dean, S. DeBeer, B. M. Hoffman, P. L. Holland and L. C. Seefeldt, *Science*, 2021, **371**, eabe5481; (*g*) K. Wonchull, C. C. Lee, A. J. Jasniewski, M. W. Ribbe and Y. Hu, *Science*, 2021, **371**, eabe5856.

14 This has pushed several groups to explore the influence of inter- or intramolecular acidic or basic functions to mimic secondary-sphere interactions: (*a*) P. Bhattacharya, D. E. Prokopchuk and M. T. Mock, *Coord. Chem. Rev.*, 2017, **334**, 67–83; (*b*) S. E. Creutz and J. C. Peters, *Chem. Sci.*, 2017, **8**, 2321–2328.

15 (*a*) J. C. Slootweg and A. R. Jupp, *Frustrated Lewis Pairs*, Springer Nature, 2020; (*b*) D. W. Stephan, *Science*, 2016, **354**, aaf7229; (*c*) D. W. Stephan, *Acc. Chem. Res.*, 2015, **48**,


© 2023 The Author(s). Published by the Royal Society of Chemistry

Open Access Article. Published on 21 November 2023. Downloaded on 1/25/2026 10:50:51 AM. This article is licensed under a Creative Commons Attribution-NonCommercial 3.0 Unported Licence.

306–316; (*d*) D. W. Stephan and G. Erker, *Angew. Chem., Int. Ed.*, 2015, **54**, 6400–6441; (*e*) *Frustrated Lewis Pairs I: Uncovering and Understanding*, ed. G. Erker and D. W. Stephan, Springer Berlin Heidelberg, 2013; (*f*) *Frustrated Lewis Pairs II: Expanding the Scope*, ed. G. Erker and D. W. Stephan, Springer Berlin Heidelberg, 2013; (*g*) D. W. Stephan and G. Erker, *Angew. Chem., Int. Ed.*, 2010, **49**, 46–76.

16 Zhu and colleagues proposed a series of *in silico* models, see: (*a*) J. Zhu, *Chem.–Asian J.*, 2019, **14**, 1413–1417; (*b*) A. M. Rouf, Y. Huang, S. Dong and J. Zhu, *Inorg. Chem.*, 2021, **60**, 5598–5606; (*c*) C. Dai, Y. Huang and J. Zhu, *Organometallics*, 2022, **41**, 1480–1487; (*d*) J. Zeng, R. Qiu and J. Zhu, *Chem.–Asian J.*, 2023, **18**, e202201236.

17 R. L. Melen, *Angew. Chem., Int. Ed.*, 2018, **57**, 880–882.

18 C. Tang, Q. Liang, A. R. Jupp, T. C. Johnstone, R. C. Neu, D. Song, S. Grimme and D. W. Stephan, *Angew. Chem., Int. Ed.*, 2017, **56**, 16588–16592.

19 L. L. Cao, J. Zhou, Z.-W. Qu and D. W. Stephan, *Angew. Chem., Int. Ed.*, 2019, **58**, 18487–18491.

20 (*a*) A. Coffinet, D. Specklin, L. Vendier, M. Etienne and A. Simonneau, *Chem.–Eur. J.*, 2019, **25**, 14300–14303; (*b*) A. Coffinet, D. Zhang, L. Vendier, S. Bontemps and A. Simonneau, *Dalton Trans.*, 2021, **50**, 5582–5589; (*c*) A. Coffinet, D. Specklin, Q. Le Dé, S. Bennaamane, L. Muñoz, L. Vendier, E. Clot, N. Mézailles and A. Simonneau, *Chem.–Eur. J.*, 2023, **29**, e202203774.

21 (*a*) C. Sivasankar, P. K. Madarasi and M. Tamizmani, *Eur. J. Inorg. Chem.*, 2020, 1383–1395; (*b*) M. Hölscher and W. Leitner, *Chem.–Eur. J.*, 2017, **23**, 11992–12003.

22 Selected examples: (*a*) A. Sacco and M. Rossi, *Inorg. Chim. Acta*, 1968, **2**, 127–132; (*b*) L. J. Archer and T. A. George, *Inorg. Chem.*, 1979, **18**, 2079–2082; (*c*) D. G. H. Hetterscheid, B. S. Hanna and R. R. Schrock, *Inorg. Chem.*, 2009, **48**, 8569–8577; (*d*) H. Fong, M.-E. Moret, Y. Lee and J. C. Peters, *Organometallics*, 2013, **32**, 3053–3062.

23 G. C. Welch and D. W. Stephan, *J. Am. Chem. Soc.*, 2007, **129**, 1880–1881.

24 (*a*) M. Tamizmani and C. Sivasankar, *Eur. J. Inorg. Chem.*, 2017, **2017**, 4239–4245; (*b*) L. R. Doyle, A. J. Wooles and S. T. Liddle, *Angew. Chem., Int. Ed.*, 2019, **58**, 6674–6677.

25 Uranium nitride was shown to be hydrogenated in the presence of borane *via* an FLP-related mechanism: L. Chatelain, E. Louyriac, I. Douair, E. Lu, F. Tuna, A. J. Wooles, B. M. Gardner, L. Maron and S. T. Liddle, *Nat. Commun.*, 2020, **11**, 337.

26 F. F. Martins and V. Krewald, *Eur. J. Inorg. Chem.*, 2023, e202300268.

27 A bis(borane) adduct of a side-on Sm–$N_2$ complex was reported recently. However, it is not clear whether the reduction of dinitrogen in this complex is the result of bis(borane) coordination *via* a push–pull mechanism, or occurs through capture by Sm prior to interaction with bis(borane). S. Xu, L. A. Essex, J. Q. Nguyen, P. Farias, J. W. Ziller, W. H. Harman and W. J. Evans, *Dalton Trans.*, 2021, **50**, 15000–15002.

28 Diborane(**4**) compound $B_2Br_4(SMe_2)_2$ has also been explored for $N_2$ functionalisation and furnishes boranylboryldiazenido complexes: L. C. Haufe, M. Arrowsmith, M. Dietz, A. Gärtner, R. Bertermann and H. Braunschweig, *Dalton Trans.*, 2022, **51**, 12786–12790.

29 Selected examples of structurally characterized group 6 hydrazido complexes: (*a*) G. A. Heath, R. Mason and K. M. Thomas, *J. Am. Chem. Soc.*, 1974, **96**, 259–260; (*b*) M. Hidai, T. Kodama, M. Sato, M. Harakawa and Y. Uchida, *Inorg. Chem.*, 1976, **15**, 2694–2697; (*c*) J. E. Barclay, A. Hills, D. L. Hughes, G. J. Leigh, C. J. Macdonald, M. A. Bakar and H. Mohd.-Ali, *J. Chem. Soc., Dalton Trans.*, 1990, 2503–2507; (*d*) D. V. Yandulov and R. R. Schrock, *Inorg. Chem.*, 2005, **44**, 1103–1117; (*e*) K. Arashiba, Y. Miyake and Y. Nishibayashi, *Nat. Chem.*, 2011, **3**, 120–125.

30 For two-fold $N_\beta$ covalent functionalisation with main group electrophiles, see: (*a*) H. Oshita, Y. Mizobe and M. Hidai, *Chem. Lett.*, 1990, 1303–1306; (*b*) H. Oshita, Y. Mizobe and M. Hidai, *Organometallics*, 1992, **11**, 4116–4123; (*c*) H. Oshita, Y. Mizobe and M. Hidai, *J. Organomet. Chem.*, 1993, **456**, 213–220; (*d*) M.-E. Moret and J. C. Peters, *J. Am. Chem. Soc.*, 2011, **133**, 18118–18121; (*e*) P. A. Rudd, N. Planas, E. Bill, L. Gagliardi and C. C. Lu, *Eur. J. Inorg. Chem.*, 2013, **2013**, 3898–3906; (*f*) D. L. M. Suess and J. C. Peters, *J. Am. Chem. Soc.*, 2013, **135**, 4938–4941; (*g*) Q. Liao, N. Saffon-Merceron and N. Mézailles, *Angew. Chem., Int. Ed.*, 2014, **53**, 14206–14210; (*h*) Q. Liao, N. Saffon-Merceron and N. Mézailles, *ACS Catal.*, 2015, **5**, 6902–6906.

31 L. Greb, *Chem.–Eur. J.*, 2018, **24**, 17881–17896.

32 (*a*) V. C. Williams, W. E. Piers, W. Clegg, M. R. J. Elsegood, S. Collins and T. B. Marder, *J. Am. Chem. Soc.*, 1999, **121**, 3244–3245; (*b*) P. A. Chase, L. D. Henderson, W. E. Piers, M. Parvez, W. Clegg and M. R. J. Elsegood, *Organometallics*, 2006, **25**, 349–357; (*c*) V. C. Williams, C. Dai, Z. Li, S. Collins, W. E. Piers, W. Clegg, M. R. J. Elsegood and T. B. Marder, *Angew. Chem., Int. Ed.*, 1999, **38**, 3695–3698; (*d*) S. P. Lewis, N. J. Taylor, W. E. Piers and S. Collins, *J. Am. Chem. Soc.*, 2003, **125**, 14686–14687; (*e*) S. P. Lewis, L. D. Henderson, B. D. Chandler, M. Parvez, W. E. Piers and S. Collins, *J. Am. Chem. Soc.*, 2005, **127**, 46–47; (*f*) S. P. Lewis, J. Chai, S. Collins, T. J. J. Sciarone, L. D. Henderson, C. Fan, M. Parvez and W. E. Piers, *Organometallics*, 2009, **28**, 249–263.

33 For related compounds whose $^{11}B$ resonances could not be detected, see ref. 12*g*, 20*a*, 20*b*, 28 and (*a*) A. Rempel, S. K. Mellerup, F. Fantuzzi, A. Herzog, A. Deißenberger, R. Bertermann, B. Engels and H. Braunschweig, *Chem.–Eur. J.*, 2020, **26**, 16019–16027; (*b*) A. Bouammali, A. Coffinet, L. Vendier and A. Simonneau, *Dalton Trans.*, 2022, **51**, 10697–10701. Other unrelated diamagnetic boron species that are NMR silent can be found in: (*c*) J. M. Farrell and D. W. Stephan, *Angew. Chem., Int. Ed.*, 2015, **54**, 5214–5217; (*d*) L. Zhu and R. Kinjo, *Angew. Chem., Int. Ed.*, 2023, **62**, e202306519.

© 2023 The Author(s). Published by the Royal Society of Chemistry

Open Access Article. Published on 21 November 2023. Downloaded on 1/25/2026 10:50:51 AM.
This article is licensed under a Creative Commons Attribution-NonCommercial 3.0 Unported Licence.

34 A $N_2$-derived titanium nitride was shown to undergo similar *N*-borylation through $C_6F_5$ group transfer: Z. Mo, T. Shima and Z. Hou, *Angew. Chem., Int. Ed.*, 2020, **59**, 8635–8644.
35 For a review on $N_2$ borylation, see: A. Simonneau, *New J. Chem.*, 2021, **45**, 9294–9301.
36 C. Y. Legault, *CYLview20*, **http://www.cylview.org** 2020.
37 A. V. Zemskov, G. N. Rodionova, Yu. G. Tuchin and V. V. Karpov, *J. Appl. Spectrosc.*, 1988, **49**, 1020–1024.
38 H. Ishino, Y. Ishii and M. Hidai, *Chem. Lett.*, 1998, **27**, 677–678.
39 Related bis-diphosphine group 6 NO complexes were shown to activate $H_2$ with the same first sphere isomerisation: A. Dybov, O. Blacque and H. Berke, *Eur. J. Inorg. Chem.*, 2010, 3328–3337.
40 P. Pyykkö and M. Atsumi, *Chem.–Eur. J.*, 2009, **15**, 12770–12779.
41 Z. Hussain, Y. Luo, Y. Wu, Z. Qu, S. Grimme and D. W. Stephan, *J. Am. Chem. Soc.*, 2023, **145**, 7101–7106.
42 F. Reiß, A. Schulz and A. Villinger, *Chem.–Eur. J.*, 2014, **20**, 11800–11811.
43 F. Tuczek, K. H. Horn and N. Lehnert, *Coord. Chem. Rev.*, 2003, **245**, 107–120.
44 (*a*) W. H. Bernskoetter, E. Lobkovsky and P. J. Chirik, *Organometallics*, 2005, **24**, 6250–6259; (*b*) R. P. Yu, J. M. Darmon, S. P. Semproni, Z. R. Turner and P. J. Chirik, *Organometallics*, 2017, **36**, 4341–4343; (*c*) S. M. Rummelt, H. Zhong, N. G. Léonard, S. P. Semproni and P. J. Chirik, *Organometallics*, 2019, **38**, 1081–1090.
45 M. M. Deegan and J. C. Peters, *Chem. Sci.*, 2018, **9**, 6264–6270.


© 2023 The Author(s). Published by the Royal Society of Chemistry